Journal of Sound and Vibration (1999) **223**(4), 611–644
Article No. jsvi.1998.2136, available online at http://www.idealibrary.com on IDEAL®

A NON-DIMENSIONAL PARAMETRIC STUDY OF ENHANCED ACTIVE CONSTRAINED LAYER DAMPING TREATMENTS

YANNING LIU AND K. W. WANG

Structural Dynamics and Controls Laboratory, Mechanical Engineering Department, The Pennsylvania State University, University Park, PA 16802, *U.S.A.*

(*Received* 9 *June* 1998, *and in final form* 14 *December* 1998)

The purpose of this research is to extend the previous work of Liao and Wang [1, 2] (*Journal of Smart Materials and Structures* **5**, 638–648; *Journal of Vibration and Acoustics* **120**, 894–900) on the Enhanced Active Constrained Layer (EACL) damping treatments and provide more comprehensive results that can be better generalized. For given strain distributions in the host structure and utilizing a self-sensing control law, closed form solutions to the longitudinal motion of the active cover sheet of the EACL are derived. Active, passive, and hybrid (total) loss factors are defined to discuss the damping properties of the treatments. With a non-dimensionalized formulation, this research identifies and examines the major factors that affect the EACL damping characteristics. These factors are: the bending stiffness ratio between the host structure and the constraining layer, the offset distance of the constraining layer from the host structure, the strain distribution in the host structure, the active control gain, the characteristic length of the EACL, the Viscoelastic Material (VEM) loss factor, and the stiffness distribution of the edge elements. The effects of these factors on open-loop and closed-loop damping characteristics of the treatment are discussed. This investigation provides insights and design guidelines to generic one-dimensional EACL surface damping treatments.

1. BACKGROUND

The Active Constrained Layer (ACL) damping treatments [3–9] have been designed to improve the damping ability of the classical Passive Constrained Layer (PCL) damping configurations. A typical ACL consists of a layer of viscoelastic material (VEM) sandwiched between a base structure and an active piezoelectric (such as PZT ceramics) constraining layer. By controlling the active cover sheet, the VEM shear deformation (shear angle) can be increased and thus more energy can be dissipated. While the ACL treatments can indeed improve the system passive damping, the VEM layer degrades the active control authority of the piezoelectric actuator being applied to the base structure when compared

0022–460X/99/240611 + 34 $30.00/0

to a simple purely active system (without VEM) [7, 8]. To increase the *transmissibility* between the voltage input to the piezoelectric cover sheet and the control action applied to the base structure, Liao and Wang recently developed the Enhanced Active Constrained Layer (EACL) damping concept by adding *edge elements* to the boundaries of the piezoelectric cover sheet [1]. It has been shown that, with proper design, the edge elements can greatly increase the active control authority and robustness of the traditional ACL system, while still maintaining sufficient passive damping [1, 2].

2. PROBLEM STATEMENT AND RESEARCH OBJECTIVE

Although the effectiveness of the EACL systems has been demonstrated and some analyses have been performed to understand its characteristics, a comprehensive and generic study that examines all the basic design parameters of the treatments has not been completed. The major issues remaining to be addressed are:

(1) Studies so far have only focused on using edge elements with equal stiffness (a symmetric configuration). The characteristics of an unsymmetric treatment have not been examined. How the stiffness *distribution* of the edge elements will affect the damping properties of the system has not been investigated.

(2) The influences of various key EACL design variables, such as the location and geometry of the treatments, the material properties of the VEM and the constraining layer, the stiffness distribution of the edge elements, and the active action, on the overall system performance have not been generically quantified. Results of the previous EACL studies were derived from specific examples of host structures, such as cantilever beams. The parameter space was also limited (mainly focused on the edge element stiffness) and the formulation was not non-dimensionalized. While these investigations do have merits in showing the feasibility of the concept and providing qualitative observations, the conclusions cannot be easily generalized.

The goal of this paper is to address the above issues and conduct a fundamental and comprehensive study of generic one-dimensional EACL configurations. By assuming different strain fields in the host structure and using a self-sensing control algorithm [5, 9], closed-form solutions are derived and non-dimensionalized. The active, passive, and total system (hybrid) loss factors of the EACL damping treatment are defined, the non-dimensional parameters that affect the loss factors are identified, and their effects on the damping characteristics of the treatment are studied.

3. SYSTEM DESCRIPTION AND MODEL

In this section, the equation of the longitudinal motion of the piezoelectric layer and the corresponding boundary conditions are first derived with specified strain fields of the host structure (a one-dimensional beam structure is used in this study). Specifying a self-sensing control law, a closed form solution to the equation is then obtained.

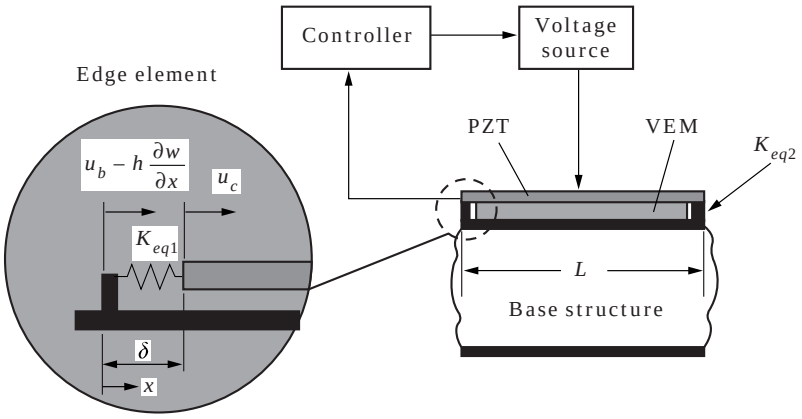

Figure 1. One-dimensional base (beam) structure with EACL treatment.

A schematic of the structural configuration is shown in Figure 1. The host structure is attached by a VEM layer, which is constrained by a layer of PZT. At the ends of the PZT, a pair of edge elements is used to connect the PZT directly to the host structure. The geometry and the material of the edge elements can be designed and selected to achieve different stiffness. The following assumptions are made in deriving the model: (1) transverse displacement w is assumed to be the same for all layers; (2) the shear strains in the PZT and the base structure are negligible and the longitudinal strain in the VEM is neglected; (3) passive damping is only considered in the shear deformation of the VEM; (4) interfaces are perfect, no slip occurs between the layers; (5) the displacement (δ) between the edge element location on the base beam and the corresponding end of the PZT layer is zero; (6) applied voltage is assumed to be uniform along the PZT; (7) only harmonic, steady state vibration is considered; (8) linear theories of elasticity, viscoelasticity, and piezoelectricity are used.

From Figure 2, the following kinematics relationship can be derived:

$$\gamma = \left(u_c - u_b + h\frac{\partial w}{\partial x}\right)/h_s, \tag{1}$$

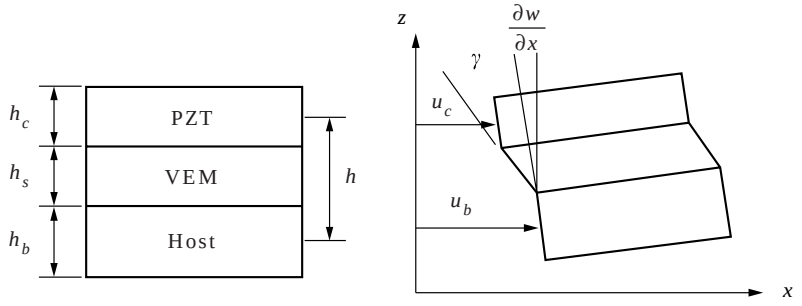

Figure 2. Kinematics relationship between γ, w, u_c and u_b.

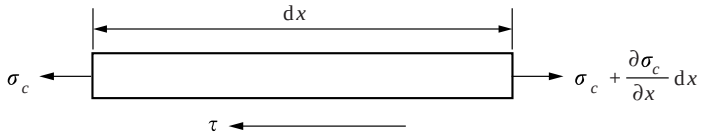

Figure 3. Free-body diagram of PZT.

with

$$h = h_b/2 + h_s + h_c/2; \tag{2}$$

γ is the shear strain in the VEM, u_c and u_b are the average longitudinal displacements of the PZT and the host structure respectively.

Figure 3 shows the free-body diagram of the PZT. Applying Newton's second law and assuming quasi-static in the axial direction of the PZT leads to

$$\frac{\partial \sigma_c}{\partial x} - \frac{\tau}{h_c} = 0. \tag{3}$$

From the constitutive equation of the piezoelectric material, the stress σ_c can be written as

$$\sigma_c = E_c\left(\frac{\partial u_c}{\partial x} - \Lambda\right). \tag{4}$$

Λ is the free strain of the PZT and can be written as

$$\Lambda = d_{31}(V/h_c). \tag{5}$$

Here, V is the control voltage applied to the PZT and d_{31} is the piezoelectric constant.

In steady state, the shear stress in equation (3) can be expressed as

$$\tau = G_s^*\gamma = G_1(1 + \mathrm{i}\eta)\gamma, \tag{6}$$

where G_s^* is the complex shear modulus of the VEM, G_1 is the storage shear modulus, and η is the material loss factor.

Substituting equations (4) and (6) into equation (3) and considering the kinematics relationship (1) yields the equilibrium equation of the longitudinal displacement of the PZT:

$$\frac{\partial^2 u_c}{\partial x^2} - \frac{G_s^*}{E_c h_c h_s}u_c = -\frac{G_s^*}{E_c h_c h_s}\left(u_b - h\frac{\partial w}{\partial x}\right), \tag{7}$$

Two boundary conditions are needed to solve for u_c. Modelling the edge elements to be longitudinal springs with equivalent stiffness K_{eq1} (left end) and K_{eq2} (right end), as shown in Figure 1, the following boundary conditions can be derived:

$$\frac{\partial u_c}{\partial x} - \Lambda - \frac{K_{eq1}}{E_c A_c}\left(u_c - u_b + h\frac{\partial w}{\partial x}\right) = 0, \quad \text{at} \quad x = 0; \tag{8}$$

$$\frac{\partial u_c}{\partial x} - \Lambda + \frac{K_{eq2}}{E_c A_c}\left(u_c - u_b + h\frac{\partial w}{\partial x}\right) = 0, \quad \text{at} \quad x = L. \tag{9}$$

It is worth noting that the equilibrium equation (7) governing the PZT longitudinal motion of the EACL treatment is the same as that of the ACL or PCL system. However, the boundary conditions for the EACL are quite different due to the edge elements. When $K_{eq1} = K_{eq2} = 0$, equations (8) and (9) will reduce to the ACL boundary conditions. Further, if no control voltage is applied, the strain at the boundaries of the PZT will be zero, and equations (8) and (9) become the boundary conditions of the PCL treatment. By adjusting the control gain and the edge element stiffness, the boundary control characteristics of the EACL treatment can be tuned to give the best damping ability.

Equations (7)–(9) can be non-dimensionalized as

$$\frac{\partial^2 \bar{u}_c}{\partial \bar{x}^2} - \Gamma^{*2}\bar{u}_c = -\Gamma^{*2}\left(\bar{u}_b - \theta_h \frac{\partial \bar{w}}{\partial \bar{x}}\right), \tag{10}$$

$$\frac{\partial \bar{u}_c}{\partial \bar{x}} - \Lambda - K_1\left(\bar{u}_c - \bar{u}_b + \theta_h \frac{\partial \bar{w}}{\partial \bar{x}}\right) = 0, \quad \text{at} \quad \bar{x} = 0; \tag{11}$$

$$\frac{\partial \bar{u}_c}{\partial \bar{x}} - \Lambda + K_2\left(\bar{u}_c - \bar{u}_b + \theta_h \frac{\partial \bar{w}}{\partial \bar{x}}\right) = 0, \quad \text{at} \quad \bar{x} = 1; \tag{12}$$

where

$$\bar{x} = x/L, \quad \theta_h = h/L, \quad \Gamma^{*2} = G_s^* L^2/E_c h_c h_s, \quad K_1 = K_{eq1} L/E_c A_c, \tag{13–16}$$

$$K_2 = K_{eq2} L/E_c A_c, \quad \bar{u}_c = u_c/L, \quad \bar{u}_b = u_b/L, \quad \bar{w} = w/L. \tag{17–20}$$

Γ^* is the non-dimensional complex characteristic length of the surface damping treatment. It combines the effects of the material properties and geometry of the treatment. For the traditional PCL, the damping property of the treatment is uniquely determined by Γ^* [10]. For the ACL, its damping property is also related to the free strain Λ of the constraining layer or the control method since the boundary conditions are not trivial as in the case of PCL. For the EACL, non-dimensional edge element stiffness K_1 and K_2 make the boundary conditions

TABLE 1

System nominal parameters

A_b	90 mm^2	E_c	6.49×10^{10} N/m^2
A_s	15 mm^2	h_b	3 mm
A_c	15 mm^2	h_s	0·5 mm
E_b	$7{\cdot}1 \times 10^{10}$ N/m^2	h_c	0·5 mm
G_s	$4{\cdot}5(1 + \mathrm{i}) \times 10^5$ N/m^2	L	250 mm

even more complex than the ACL. But this also gives us the flexibility to design Λ, K_1 and K_2 and achieve the best damping property of the system, as will be seen later. All parameters used in this paper are listed in Table 1 unless stated otherwise.

In this paper, a host structure with the EACL treatment on both sides is considered. With this arrangement, the neutral axis of the composite beam will always remain at the mid-section of the host beam. Therefore, the strain in the host structure (note that only the strain field of the base structure directly beneath the VEM layer is of interest in this analysis) can be approximated as

$$\varepsilon(\bar{x}, \bar{z}) = (A\bar{x} + B)\bar{z}. \tag{21}$$

In the above expression, A and B are constants. The strain ε is assumed to vary sinusoidally over time due to the cyclic vibration of the system and change linearly in space. When A is equal to zero, the strain along the base structure is constant and symmetrical about the mid-section of the PZT. When A is equal to $-2B$, the strain field is anti-symmetrical about the mid-section of the PZT. The values of A and B are not important here since only the A to B ratio will affect the loss factors (see next section). In this paper, the constant B is set to be $-0{\cdot}1$. The constant A can change from 0 to 0·2 so that the strain field of the host structure varies from a symmetrical distribution to an anti-symmetrical distribution. This is equivalent to consider the effects of the location of the EACL and the vibration mode of the host structure. For example, the antisymmetrical strain distribution corresponds to the case that the treatment covers a nodal point of a vibration mode and the nodal point happens to be located in the middle of the treatment. As long as the length of the EACL treatment is less than the half wavelength of the vibration modes of interest, a certain A and B combination can always be found to approximate the location of the treatment. Otherwise, a higher-order polynomial has to be used to approximate the strain field. Integrating equation (21) with respect to x and considering that there is no shear strain in the base beam, the following two equations can be derived:

$$\bar{u}_b = 0, \quad \frac{\partial \bar{w}}{\partial \bar{x}} = -\left(\frac{A}{2}\bar{x}^2 + B\bar{x} + C\right). \tag{22, 23}$$

The constant C is not important in our discussion here since it will be cancelled in the final equations of the loss factors.

Substituting equations (22) and (23) into equation (10) gives

$$\bar{u}_c = \theta_h\left(C_1 \cosh(\Gamma^*\bar{x}) + C_2 \sinh(\Gamma^*\bar{x}) + \frac{A}{2}\bar{x}^2 + B\bar{x} + C + \frac{A}{\Gamma^{*2}}\right). \tag{24}$$

The constants C_1 and C_2 will be determined by the boundary conditions of the PZT.

Substituting equations (22)–(24) into equation (1), the shear γ in the viscoelastic layer becomes

$$\gamma = \frac{\theta_h}{\theta_s}\left(C_1 \cosh(\Gamma^* \bar{x}) + C_2 \sinh(\Gamma^* \bar{x}) + \frac{A}{\Gamma^{*2}}\right), \tag{25}$$

where θ_s is the non-dimensional viscoelastic layer thickness defined as

$$\theta_s = h_s/L. \tag{26}$$

To solve for the constants C_1 and C_2, the free strain Λ of the PZT, which depends on the control law, has to be determined first. In this paper, the self-sensing algorithm proposed by Shen [9] and Baz [5] is used:

$$\Lambda = K_g[\dot{u}_c(0, t) - \dot{u}_c(L, t)] = \mathrm{i}\omega K_g L[\bar{u}_c(0, t) - \bar{u}_c(1, t)] = \mathrm{i}G[\bar{u}_c(0, t) - \bar{u}_c(1, t)]. \tag{27}$$

Here G is the non-dimensional control gain defined as $K_g \omega L$. ω is the frequency in radians, and K_g is the practical control gain. While more sophisticated control laws can also be employed, using this simple scheme will help us gain better insight from the analytical results.

Substituting equations (22)–(24), and (27) into equations (11) and (12) gives the following algebraic equations for solving the constants C_1 and C_2:

$$\begin{bmatrix} \mathrm{i}G(\cosh\Gamma^* - 1) - K_1 & \Gamma^* + \mathrm{i}G\sinh\Gamma^* \\ \Gamma^*\sinh\Gamma^* + \mathrm{i}G(\cosh\Gamma^* - 1) + K_2\cosh\Gamma^* & \Gamma^*\cosh\Gamma^* + \mathrm{i}G\sinh\Gamma^* + K_2\sinh\Gamma^* \end{bmatrix} \begin{Bmatrix} C_1 \\ C_2 \end{Bmatrix} = \begin{Bmatrix} d_1 \\ d_2 \end{Bmatrix}, \tag{28}$$

$$d_1 = -B - \mathrm{i}G\left[\frac{A}{2} + B\right] + K_1\frac{A}{\Gamma^{*2}}, \quad d_2 = -A - B - \mathrm{i}G\left[\frac{A}{2} + B\right] - K_2\frac{A}{\Gamma^{*2}}. \tag{29, 30}$$

It can be seen from equations (28)–(30) that the constants C_1 and C_2 are the functions of the control gain (G), the complex characteristic length (Γ^*), the strain distribution in the host structure (A, B), and the stiffness distribution of the edge elements (K_1, K_2).

4. LOSS FACTORS OF THE EACL TREATMENT

The energies dissipated per cycle by active control (W_a) and by passive damping (W_p) can be expressed as [5, 9]

$$W_a = 2\pi G E_c A_c L[\bar{u}_c(0) - \bar{u}_c(1)]^2, \quad W_p = 2\pi\eta G_1 A_s L\int_0^1 \gamma^2 \,\mathrm{d}\bar{x}. \tag{31, 32}$$

Considering equations (24) and (25), W_a and W_p can be expressed as

$$W_a = 2\pi G E_c A_c L\theta_h^2\left[C_1(\cosh\Gamma^* - 1) + C_2\sinh\Gamma^* + \frac{A}{2} + B\right]^2, \tag{33}$$

$$W_p = 2\pi\eta E_c A_c L\theta_h^2 \,\mathrm{Re}(\Gamma^{*2}) \int_0^1 \left[C_1 \cosh \Gamma^* \bar{x} + C_2 \sinh \Gamma^* \bar{x} + \frac{A}{\Gamma^{*2}}\right]^2 \mathrm{d}\bar{x}. \tag{34}$$

The active loss factor η_a and passive loss factor η_p of the EACL treatment are defined as

$$\eta_a = \frac{W_a}{2\pi W_s}, \quad \eta_p = \frac{W_p}{2\pi W_s}, \tag{35, 36}$$

where W_s is the maximum strain energy stored in the PZT, VEM, the edge elements, and the host structure between the treatments:

$$\begin{aligned} W_s = {} & \frac{E_b b L^2}{2} \int_0^1 \int_{-\theta_b/2}^{\theta_b/2} \varepsilon^2(\bar{x}, \bar{z}) \,\mathrm{d}\bar{z} \,\mathrm{d}\bar{x} + E_c b L^2 \int_0^1 \int_{-\theta_c/2}^{\theta_c/2} \left[\frac{\partial \bar{u}_c}{\partial \bar{x}} - \bar{z}_c \frac{\partial^2 \bar{w}}{\partial \bar{x}}\right]^2 \mathrm{d}\bar{z}_c \,\mathrm{d}\bar{x} \\ & + G_1 b h_s L \int_0^1 \gamma^2 \,\mathrm{d}\bar{x} + K_{eq1} L^2 \left[\bar{u}_c - \bar{u}_b + \theta_h \frac{\partial \bar{w}}{\partial \bar{x}}\right]_{\bar{x}=0}^2 \\ & + K_{eq2} L^2 \left[\bar{u}_c - \bar{u}_b + \theta_h \frac{\partial \bar{w}}{\partial \bar{x}}\right]_{\bar{x}=1}^2. \end{aligned} \tag{37}$$

Considering equations (21)–(25), W_s can be written in the form

$$W_s = E_c A_c L \theta_h^2 f_n(A, B, K_1, K_2, G, \Gamma^*, EI, \Delta), \tag{38}$$

where

$$\begin{aligned} f_n = {} & \frac{2 + EI}{24\Delta^2}\left(\frac{A^2}{3} + AB + B^2\right) \\ & + \int_0^1 [C_1 \Gamma^* \sinh(\Gamma^* \bar{x}) + C_2 \Gamma^* \cosh(\Gamma^* \bar{x}) + A\bar{x} + B]^2 \,\mathrm{d}\bar{x} + K_1 \left[C_1 + \frac{A}{\Gamma^{*2}}\right]^2 \\ & + \mathrm{Re}(\Gamma^{*2}) \int_0^1 \left[C_1 \cosh(\Gamma^* \bar{x}) + C_2 \sinh(\Gamma^* \bar{x}) + \frac{A}{\Gamma^{*2}}\right]^2 \mathrm{d}\bar{x} \\ & + K_2 \left[C_1 \cosh \Gamma^* + C_2 \sinh \Gamma^* + \frac{A}{\Gamma^{*2}}\right]^2, \end{aligned} \tag{39}$$

$$EI = \frac{E_b I_b}{E_c I_c}, \quad \Delta = \frac{\theta_h}{\theta_c} = \frac{h}{h_c}. \tag{40, 41}$$

EI is the ratio of the bending stiffness of the host beam and that of the PZT, Δ is the non-dimensional offset distance of the PZT from the mid-section of the host structure.

Substituting equations (31), (32) and (38) into equations (35) and (36), the active and passive loss factors can be expressed as

$$\eta_a = G\frac{\left[C_1(\cosh\Gamma^* - 1) + C_2\sinh\Gamma^* + \dfrac{A}{2} + B\right]^2}{f_n(A, B, K_1, K_2, G, \Gamma^*, EI, \Delta)}, \tag{42}$$

$$\eta_p = \eta\ \mathrm{Re}(\Gamma^{*2})\frac{\displaystyle\int_0^1\left[C_1\cosh\Gamma^*\bar{x} + C_2\sinh\Gamma^*\bar{x} + \frac{A}{\Gamma^{*2}}\right]^2 \mathrm{d}x}{f_n(A, B, K_1, K_2, G, \Gamma^*, EI, \Delta)}. \tag{43}$$

The total system (hybrid) loss factor of the EACL treatment η_s is the summation of the active and passive loss factors.

$$\eta_s = \eta_a + \eta_p. \tag{44}$$

From equations (42) and (43), it is found that many factors will affect the damping properties of the EACL treatment. Considering equation (28), the active and passive loss factors can be written in the general forms

$$\eta_a = f_a(A, K_1, K_2, G, \Gamma, \eta, EI, \Delta), \quad \eta_p = f_p(A, K_1, K_2, G, \Gamma, \eta, EI, \Delta), \tag{45, 46}$$

where the complex characteristic length Γ^* is replaced by its magnitude Γ and the VEM loss factor η. One can derive from equations (42) and (43) that only the A to B ratio, and not the values of A and B, will affect the loss factors. Therefore, B is omitted in the expressions of η_a and η_p (equations (45) and (46)). The effects of some parameters, such as EI and Δ, are obvious. But the effects of other parameters are not very clear. In the following two sections, it will be examined how these parameters will influence the open-loop and closed-loop damping properties of the EACL treatment.

5. OPEN-LOOP DAMPING CHARACTERISTICS

The open-loop system is studied first (control gain $G = 0$). Such an investigation will be useful for understanding the fail-safe ability of the design. It can be seen from equation (46) that, except the bending stiffness ratio EI and the offset distance Δ, the open-loop loss factor $\eta_{op}(= \eta_p)$ is affected by four factors: the VEM loss factor η, the strain distribution in the host structure (A), the stiffness distribution of the edge elements (K_1 and K_2), and the characteristic length (Γ). Through this analysis, it is found that parameters K_1, K_2 and Γ can be designed for each given strain field A to maximize the open-loop loss factor η_{op}. The higher the VEM loss factor, the higher the open-loop loss factor. But the VEM loss factor η will not affect the optimal selection of K_1, K_2, and Γ. The details are presented in the following paragraphs.

For a symmetrical and constant strain field ($A = 0$) of the host beam, the edge elements can be used to change the optimal characteristic length Γ_{opt} of the treatment. The PCL without edge elements ($K_1 = K_2 = 0$) reaches a maximum loss factor when the characteristic length Γ equals Γ_{opt0}, as shown in Figure 4, which is consistent with Plunkett and Lee's discussion about the optimal length

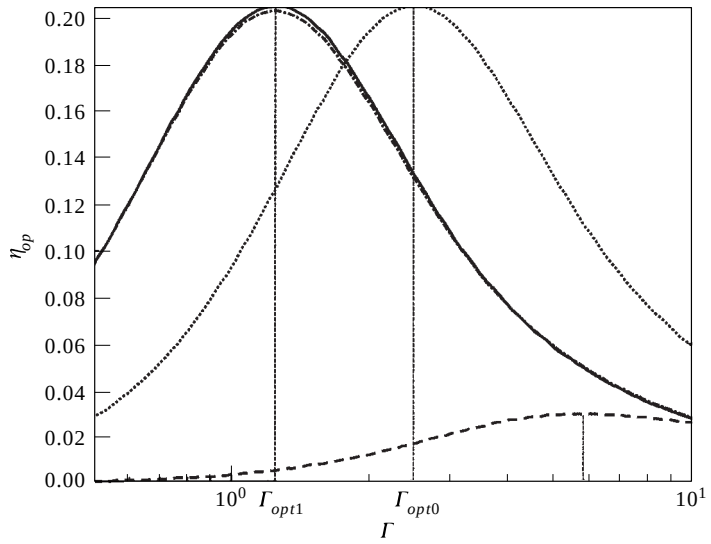

Figure 4. Open-loop loss factor η_{op} versus characteristic length Γ for the constant strain field in the host beam: ·····, $K_1 = K_2 = 0$; ——, $K_1 = \infty$, $K_2 = 0$; -·-·-·-, $K_1 = 100$, $K_2 = 0$; - - - -, $K_1 = K_2 = 5$.

of the PCL [10]. In fact, if W_s in equation (37) were defined as the maximum strain energy stored in the PZT and neglecting the shear in the VEM,

$$W_s = E_c b L^2 \int_0^1 \int_{\theta_h - \theta_c/2}^{\theta_h + \theta_c/2} \varepsilon^2(\bar{x}, \bar{z})\, \mathrm{d}\bar{z}\, \mathrm{d}\bar{x} = E_c b \theta_c L^2 \left(\theta_h^2 + \frac{\theta_c^2}{12}\right)\left(\frac{A^2}{3} + AB + B^2\right), \tag{47}$$

it can be shown that the optimal characteristic length $\Gamma_{opt0} = 3{\cdot}28$, which is exactly the number obtained by Plunkett and Lee. Increasing the stiffness of the edge elements simultaneously reduces the loss factor of the system, which is not desired here. However, an interesting and useful case is when one of the edge elements is stiff and the other is extremely soft ($K_1 \to \infty$, $K_2 = 0$; or $K_1 = 100$, $K_2 = 0$ in Figure 4). In this case, the system has an optimal characteristic length Γ_{opt1}, which is half the length in the preceding case. This is easy to imagine because the shear strain in the VEM is zero at the mid-section and symmetrical about the mid-section when the constraining layer is free at both ends. When the constraining layer is fixed at one end, it forces the shear in the VEM to be zero at that end, just as it is in the mid-section of the preceding case ($K_1 = K_2 = 0$) [11]. Therefore, the optimal characteristic length Γ_{opt1} in this case is $\frac{1}{2}\Gamma_{opt0}$. The energy dissipated by the viscoelastic layer is half of the previous case. Since the energy stored in the system now is also half of the previous case, the maximum open-loop loss factor η_{op} remains the same, according to the definition of the open-loop loss factor. Further increasing or decreasing Γ will result in the degradation of the damping ability of the system. In Figure 5, the maximum loss factor η_{op} and its corresponding optimal characteristic length Γ_{opt} are shown for

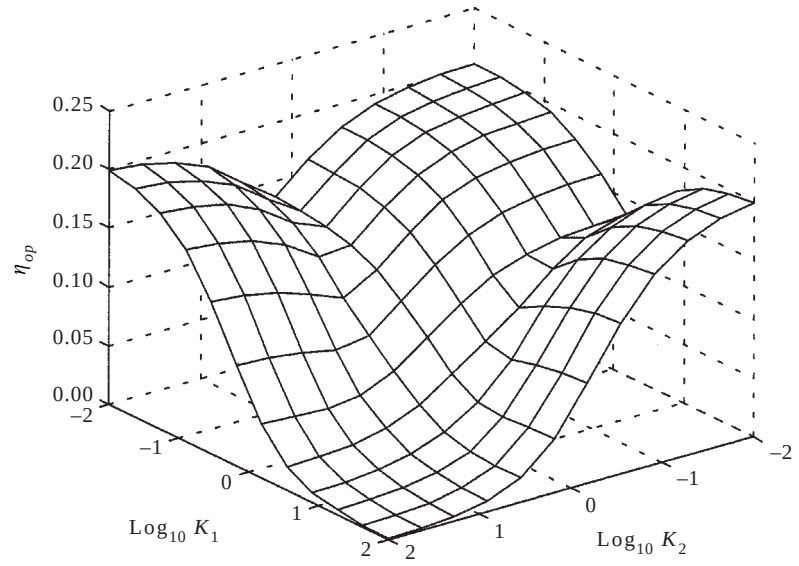

(a)

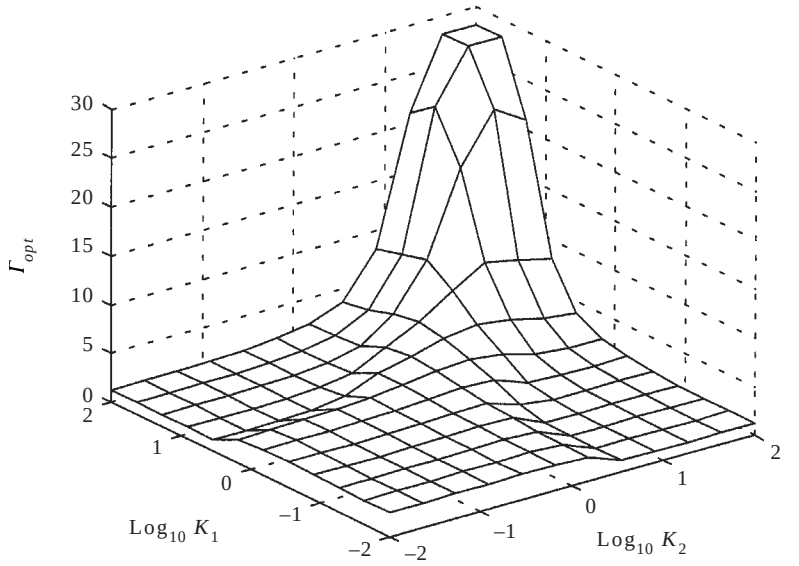

(b)

Figure 5. (a) Maximum open-loop loss factor η_{op} versus K_1 and K_2 for $A = 0$, $B = -0{\cdot}1$; (b) optimal characteristic length Γ_{opt} versus K_1 and K_2 for $A = 0$, $B = -0{\cdot}1$.

the different selections of the edge element stiffness K_1 and K_2. The loss factor η_{op} reaches almost the same maximum value when $K_1 = K_2 = 0{\cdot}01$; $K_1 = 100$, $K_2 = 0{\cdot}01$; and $K_1 = 0{\cdot}01$, $K_2 = 100$. But the optimal characteristic lengths Γ_{opt} for these cases are distinct. In some practical problems, the constrained layer treatment without edge elements might not reach the optimal characteristic length Γ_{opt} due to space constraints. The edge elements can be used to restrain

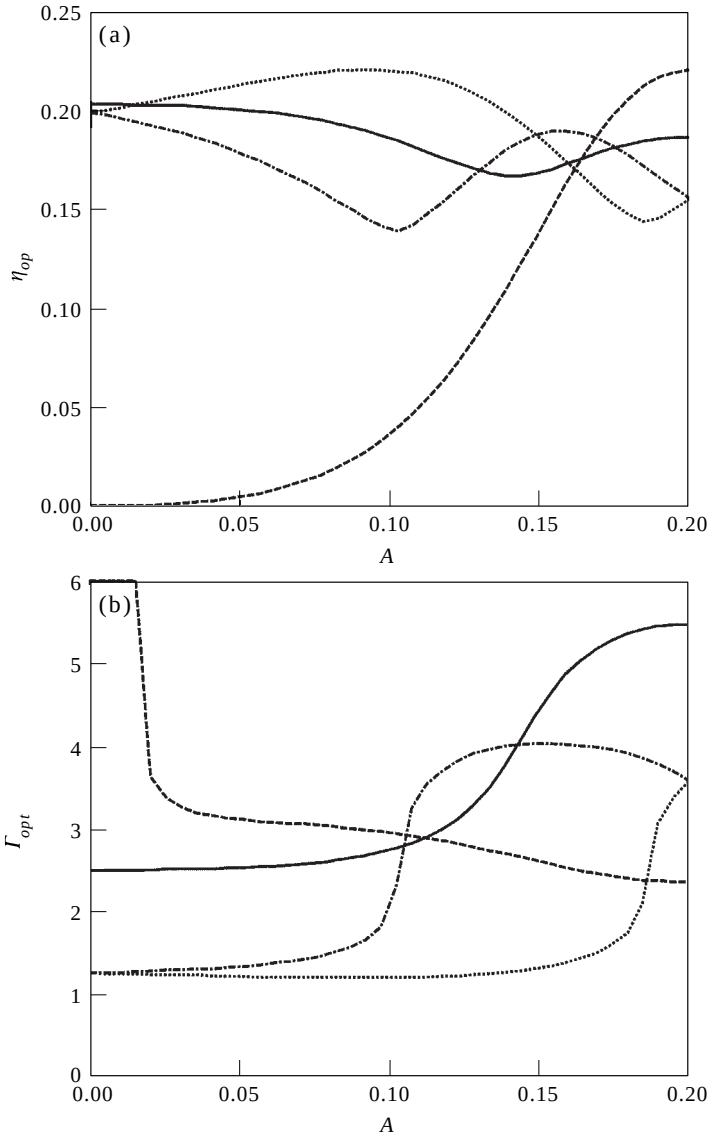

Figure 6. (a) Maximum open-loop loss factor η_{op} versus strain distribution index A; (b) optimal characteristic length Γ_{opt} versus strain distribution index A; ·····, $K_1 = 100$, $K_2 = 0{\cdot}01$; ——, $K_1 = K_2 = 0{\cdot}01$; -·-·-·-, $K_1 = 0{\cdot}01$, $K_2 = 100$; - - - -, $K_1 = K_2 = 100$.

one end of the constraining layer to bisect Γ_{opt} so that the damping property of the treatment can be improved.

Constant strain in the host structure is very unlikely to happen in reality. In most cases, the strain of the beam beneath the treatment has a certain distribution. When the strain in the host structure is not uniform, the optimal characteristic length Γ_{opt} and its corresponding maximum loss factor η_{op} will change. For each strain distribution in the host structure, there is an optimal selection of K_1, K_2 and Γ to maximize the open-loop loss factor η_{op} of the

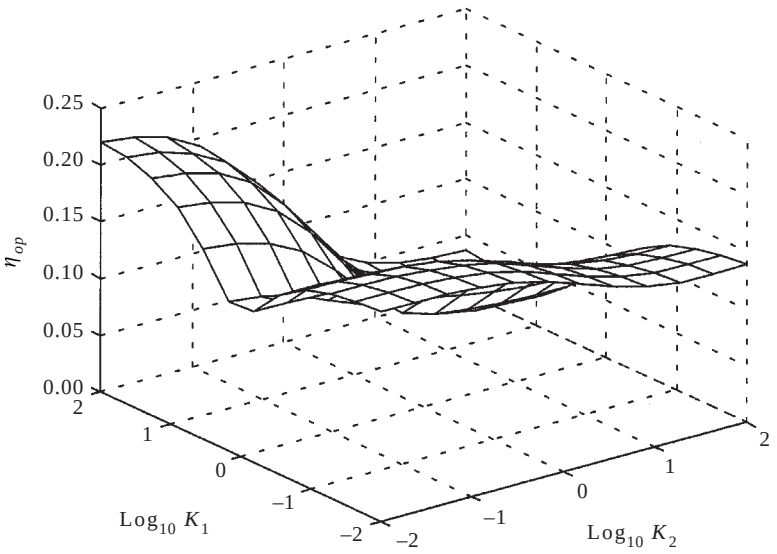

(a)

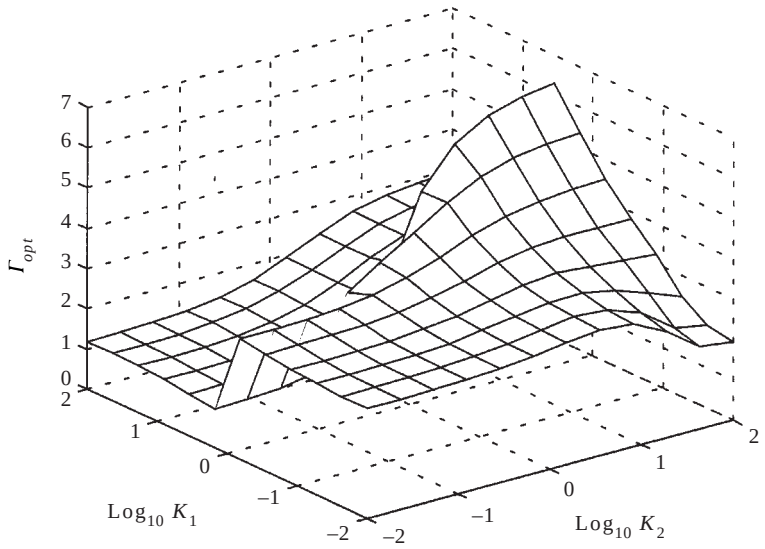

(b)

Figure 7. (a) Maximum open-loop loss factor η_{op} versus K_1 and K_2 for $A = 0{\cdot}1$, $B = -0{\cdot}1$; (b) optimal characteristic length Γ_{opt} versus K_1 and K_2 for $A = 0{\cdot}1$, $B = -0{\cdot}1$.

treatment. Using the first order approximation, the strain can be expressed linearly as shown in equation (21). In Figure 6, the maximum open-loop loss factor η_{op} and its corresponding optimal characteristic length Γ_{opt} are plotted versus strain distribution index A for the different selections of the edge element stiffness distribution. For the constrained layer treatment with very soft edge elements ($K_1 = K_2 = 0{\cdot}01$), Γ_{opt} increases and η_{op}, in general, drops slightly when the strain field changes from constant and symmetric to anti-symmetric.

Demoret and Torvik [12] also found that Γ_{opt} of the PCL without edge elements becomes larger when the strain varies away from the constant field. It is obvious from Figure 6 that the constrained layer treatment without edge elements is not the best choice when the strain field being treated is not constant. The case of $K_1 = 100$, $K_2 = 0{\cdot}01$ achieves higher damping than the other cases in a large range of A. This phenomenon is because selecting a stiffer edge element at the higher strain end has the effect of amplifying the shear strain in the viscoelastic layer [11]. When the strain field is symmetric ($A = 0$) or anti-symmetric ($A = 0{\cdot}2$), the cases of $K_1 = 100$, $K_2 = 0{\cdot}01$ and $K_1 = 0{\cdot}01$, $K_2 = 100$ obtain the same open-loop loss factor since they are essentially the same selection. To consider the effect of the stiffness distribution of the edge elements, the maximum loss factor η_{op} and the corresponding optimal characteristic length Γ_{opt} are plotted versus K_1 and K_2 for $A = 0{\cdot}1$ in Figure 7. As it shows, to have the best damping property, the most rigid K_1 ($K_1 = 100$), softest K_2 ($K_2 = 0{\cdot}01$) and Γ_{opt1} should be used. However, when the strain field being treated is anti-symmetric ($A = 0{\cdot}2$), as shown in Figure 8, the most rigid K_1 and K_2 ($K_1 = K_2 = 100$) and $\Gamma = \Gamma_{opt2}$ (this value depends on EI and Δ) should be selected to give the highest damping.

In practical applications, if the strain distribution of the host structure is approximately known, the selection of the edge element stiffness K_1 and K_2 and the optimal characteristic length Γ_{opt} can be simplified. It is worth noting from Figure 6 that when A changes from 0 to 0·1, Γ_{opt} of the cases of $K_1 = K_2 = 0{\cdot}01$ and $K_1 = 100$, $K_2 = 0{\cdot}01$ is almost unchanged. This means that when the strain in the beam is in phase or when the treatment does not cover a nodal point, the value of Γ_{opt} from the constant strain field can be used to provide the maximum damping ability to the treatment. As illustrated in Figure 6, η_{op} of the constrained layer treatment with the cover sheet constrained by the edge element at the high strain end ($K_1 = 100$, $K_2 = 0{\cdot}01$) is larger than any other cases, and Γ_{opt} remains unchanged until A is greater than 0·15. Thus, this case is more efficient and robust in dissipating system energy than others are. If the treatment has to be placed on a nodal point of a certain mode, and the nodal point has to be near the middle section of the treatment, very large K_1 and K_2 and the corresponding Γ_{opt}, as shown in Figure 8, should be used to increase the damping of this mode.

In the above studies of the selections of K_1, K_2 and Γ for the different strain fields in the host structure, the VEM loss factor η is fixed. The reason is that the VEM loss factor will not affect the selection. In Figure 9, the open-loop loss factor η_{op} versus Γ is plotted for the different VEM loss factors, when $A = 0$, $A = 0{\cdot}1$ and $A = 0{\cdot}2$, respectively. It can be seen from the figure that the open-loop loss factor can be amplified by selecting the VEM with larger loss factor. But for the different VEM loss factor, the optimal characteristic length Γ_{opt} remains the same. Therefore, in the design of the open-loop damping treatment, the VEM with the largest loss factor should first be selected. Then, K_1 and K_2 should be selected according to the strain field in the host structure. And finally, the characteristic length Γ can be optimized.

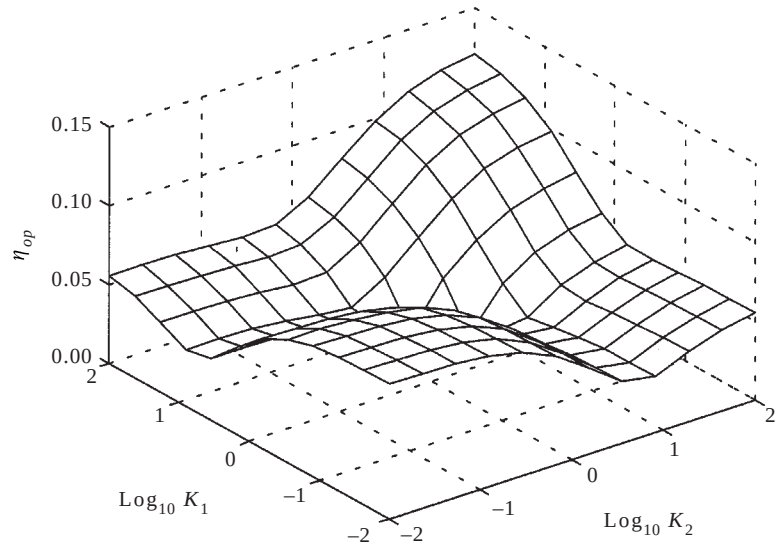

(a)

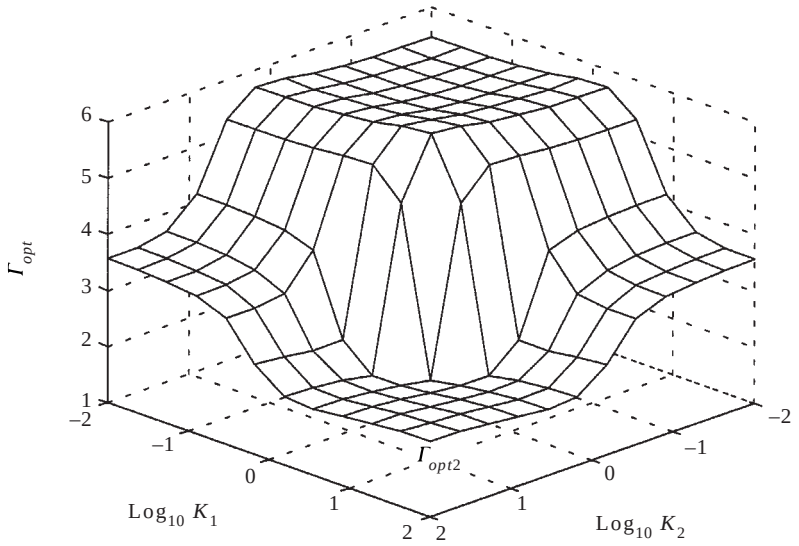

(b)

Figure 8. (a) Maximum open-loop loss factor η_{op} versus K_1 and K_2 for $A = 0{\cdot}2$, $B = -0{\cdot}1$; (b) optimal characteristic length Γ_{opt} versus K_1 and K_2 for $A = 0{\cdot}2$, $B = -0{\cdot}1$.

6. CLOSED-LOOP DAMPING CHARACTERISTICS

When a control voltage is applied to the PZT, it changes the shear strain in the VEM layer, and thus changes the system passive damping. On the other hand, such input will also direct active force and moment to the host structure and provide active damping. The total system damping (η_s) is thus a combination of active (η_a) and passive (η_p) damping actions.

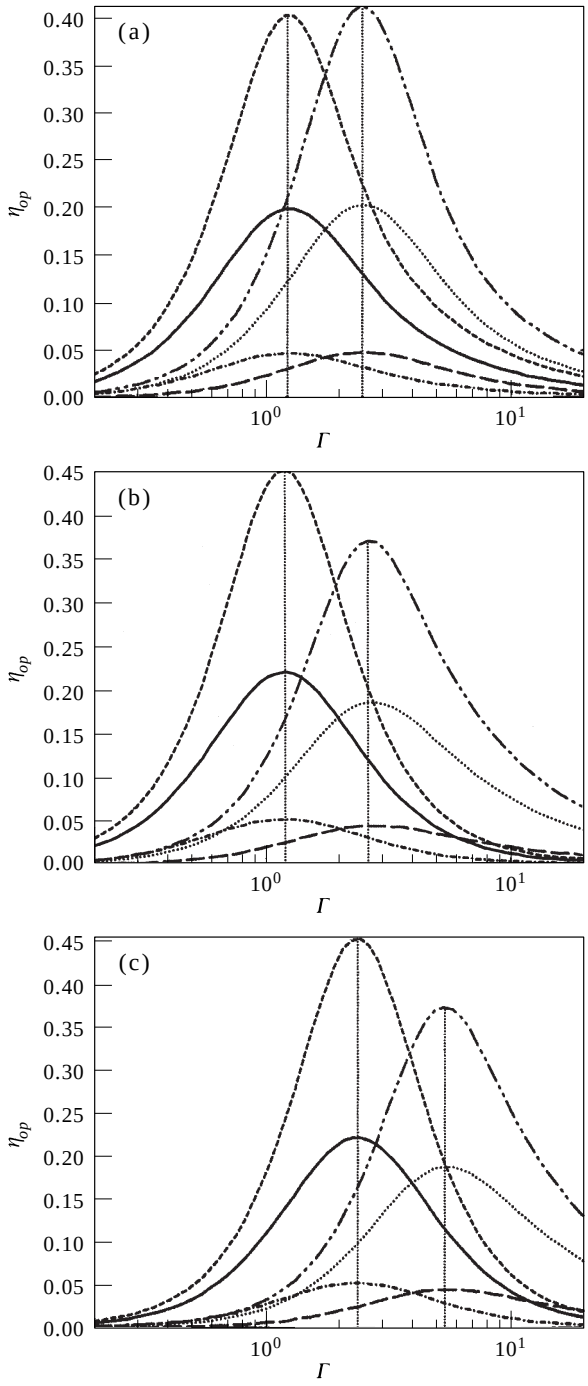

Figure 9. The open-loop loss factor η_{op} versus characteristic length Γ. (a) $A = 0$: ----, $K_1 = 100$, $K_2 = 0{\cdot}01$, $\eta = 5$; ——, $K_1 = 100$, $K_2 = 0{\cdot}01$, $\eta = 1$; -·-·-, $K_1 = 100$, $K_2 = 0{\cdot}01$, $\eta = 0{\cdot}2$; -··-··-, $K_1 = K_2 = 0{\cdot}01$, $\eta = 5$; ·····, $K_1 = K_2 = 0{\cdot}01$, $\eta = 1$; – –, $K_1 = K_2 = 0{\cdot}01$, $\eta = 0{\cdot}2$. (b) $A = 0{\cdot}1$: ----, $K_1 = 100$, $K_2 = 0{\cdot}01$, $\eta = 5$; ——, $K_1 = 100$, $K_2 = 0{\cdot}01$, $\eta = 1$; -·-·-, $K_1 = 100$, $K_2 = 0{\cdot}01$, $\eta = 0{\cdot}2$; -··-··-, $K_1 = K_2 = 0{\cdot}01$, $\eta = 5$; ·····, $K_1 = K_2 = 0{\cdot}01$, $\eta = 1$; – –, $K_1 = K_2 = 0{\cdot}01$, $\eta = 0{\cdot}2$. (c) $A = 0{\cdot}2$: ----, $K_1 = K_2 = 100$, $\eta = 5$; ——, $K_1 = K_2 = 100$, $\eta = 1$; -·-·-, $K_1 = K_2 = 100$, $\eta = 0{\cdot}2$; -··-··-, $K_1 = K_2 = 0{\cdot}01$, $\eta = 5$; ·····, $K_1 = K_2 = 0{\cdot}01$, $\eta = 1$; – –, $K_1 = K_2 = 0{\cdot}01$, $\eta = 0{\cdot}2$.

From equations (45) and (46), except EI and Δ, the closed-loop loss factor η_s will be affected by five factors: the VEM loss factor η, the strain distribution in the host structure (A), the stiffness distribution of the edge elements (K_1 and K_2), the characteristic length Γ of the treatment, and the control gain G of the system. Therefore, the effects of the six parameters A, G, K_1, K_2, Γ and η on the loss factors (η_a, η_p, η_s) need to be discussed to completely understand the closed-loop damping characteristics of the EACL treatment.

6.1. ACTIVE CONTROL ABILITY OF THE EACL TREATMENT

The effectiveness of using the edge elements to increase the active loss factor not only depends on the control gain G and the stiffness distribution of the edge elements (K_1 and K_2), but is also closely related to the strain distribution in the host structure (A) and the characteristic length of the treatment (Γ).

When the strain in the host structure is in phase ($0 \leqslant A \leqslant 0{\cdot}1$), the control gain G can be optimized to maximize the active loss factor. Figure 10 shows the effects of the control gain G and strain distribution parameter A on the active loss factor (η_a) for three selections of the edge element stiffness distribution when $\Gamma = \Gamma_{opt0}$. It can be seen clearly that there is an optimal control gain maximizing the active loss factor for non-anti-symmetric strain field. That is, higher gain does not always give more active damping. This is because of the self-sensing control algorithm used here. In fact, when G approaches infinity, equation (28) can be simplified to

$$\begin{Bmatrix} C_1 \\ C_2 \end{Bmatrix} = \begin{Bmatrix} 0 \\ -(A/2 + B)/\sinh \Gamma^* \end{Bmatrix}. \tag{48}$$

Substituting C_1 and C_2 into equation (42) and since f_n is constant in this case, η_a will approach zero.

In addition to the control gain, the stiffness distribution of the edge elements can also be optimized to magnify the active loss factor. It can also be observed from Figure 10 that the active loss factor can be increased significantly if both K_1 and K_2 are large, when A is not close to 0·2 (anti-symmetrical strain field). Take $A = 0$ and $A = 0{\cdot}1$ as examples (Figures 11(a) and (b)), increasing the edge element stiffness can enhance the active control authority, especially when K_1 and K_2 are increased simultaneously.

In the above discussions of the optimal control gain and the stiffness distribution of the edge elements, the VEM loss factor and the characteristic length Γ are fixed. It is found that the effects of Γ on the maximum active loss factor and its corresponding optimal control gain are correlated with the stiffness distribution of the edge elements. But the VEM loss factor η almost has no effect on the maximum active loss factor and the corresponding optimal control gain. In Figures 12(a)–(d), the maximum active loss factor η_a and its corresponding optimal control gain G_{opt} are plotted against the characteristic length Γ for $\eta = 0{\cdot}2$ and 1·0, when $A = 0$ and $A = 0{\cdot}1$. It can be seen from the figures that when $K_1 = 100$, $K_2 = 0{\cdot}01$, increasing Γ can enhance the active loss factor. This is because, for this case of K_1, K_2 distribution, increasing Γ can provide stronger transmissibility between the input voltage and output force, and

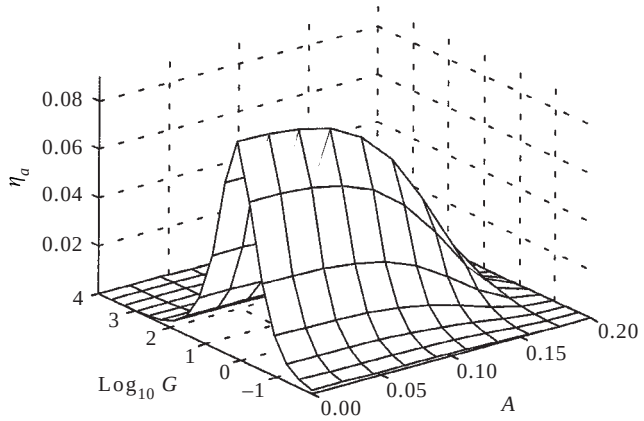

(a)

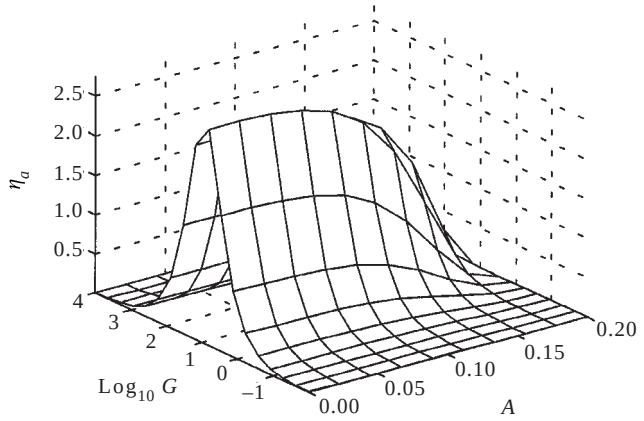

(b)

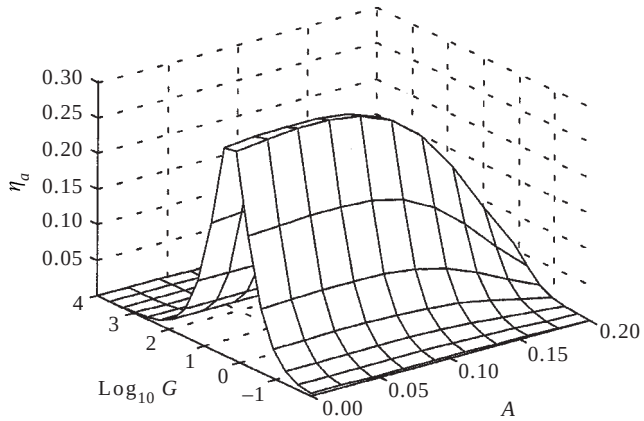

(c)

Figure 10. Active-loss factor η_a versus control gain G and strain distribution parameter A for $\Gamma = \Gamma_{opt0}$: (a) $K_1 = K_2 = 0{\cdot}01$, (b) $K_1 = K_2 = 100$, (c) $K_1 = 100$, $K_2 = 0{\cdot}01$.

thus can obtain a larger active loss factor. In this sense, Γ can be regarded as the domain factor and K_1 and K_2 as the boundary factors for determining transmissibility. When $K_1 = K_2 = 100$, the transmissibility is already high due to the edge element distribution, and thus η_a is almost independent of Γ, as shown in Figures 12(a) and (c). In both cases, the VEM loss factor η almost does not influence the maximum η_a and the optimal control gain G_{opt}. Therefore, to achieve high active control authority, the largest K_1 and K_2 should be selected, and the corresponding optimal control gain should be used.

When the strain distribution of the host structure is anti-symmetric ($A = 0{\cdot}2$), symmetric EACL ($K_1 = K_2$) cannot actively control the structure, no matter what the characteristic length and the control gain are. Unsymmetrical EACL, on the other hand, can actively control the structure. From equation (28), when $A = -2B$ and $K_1 = K_2 = K$, constants C_1 and C_2 can be expressed as

$$\begin{Bmatrix} C_1 \\ C_2 \end{Bmatrix} = B\left(1 + \frac{2K}{\Gamma^{*2}}\right) \times \begin{bmatrix} \mathrm{i}G(\cosh\Gamma^* - 1) - K & \Gamma^* + \mathrm{i}G\sinh\Gamma^* \\ \Gamma^*\sinh\Gamma^* + (\mathrm{i}G + K)\cosh\Gamma^* - \mathrm{i}G & \Gamma^*\cosh\Gamma^* + (\mathrm{i}G + K)\sinh\Gamma^* \end{bmatrix}^{-1} \times \begin{Bmatrix} -1 \\ 1 \end{Bmatrix}. \tag{49}$$

Then, it can be shown that the following equation is always true:

$$\bar{u}_c(1) - \bar{u}_c(0) = \theta_h[C_1(\cosh\Gamma^* - 1) + C_2\sinh\Gamma^*] = 0. \tag{50}$$

Since energy dissipated per cycle by active damping is proportional to the displacement difference at the ends of the PZT [9], the active loss factor is zero. That is, symmetrical EACL cannot actively control the anti-symmetrical strain field. Since the symmetrical EACL on the anti-symmetrical strain field results in the uncontrollability of the active action, the most straightforward way to avoid this is to change the position of the EACL treatment such that the strain in the host structure directly beneath the treatment is in phase ($0 \leqslant A \leqslant 0{\cdot}1$). Another possible method is to use EACL with unsymmetrical stiffness distribution of the edge elements. The active loss factor versus K_1 and K_2 for anti-symmetrical strain field ($A = 0{\cdot}2$) is plotted in Figure 11(c). The figure verifies that the active loss factor is zero when K_1 equals K_2. The more interesting phenomenon is that the unsymmetrical EACL, that is when $K_1 \neq K_2$, can actively control the anti-symmetrical strain field. The active loss factor of the treatment can be further increased by selecting optimal characteristic length, as shown in Figure 12(e). However, the active loss factor here is relatively small. This indicates that, to achieve high active control authority, the EACL should not cover the nodal points of the modes to be controlled.

6.2. PASSIVE DAMPING ABILITY OF EACL TREATMENT

Similar to the active loss factor, the effects of the control gain G and the stiffness distribution of the edge elements (K_1 and K_2) on the passive loss factor

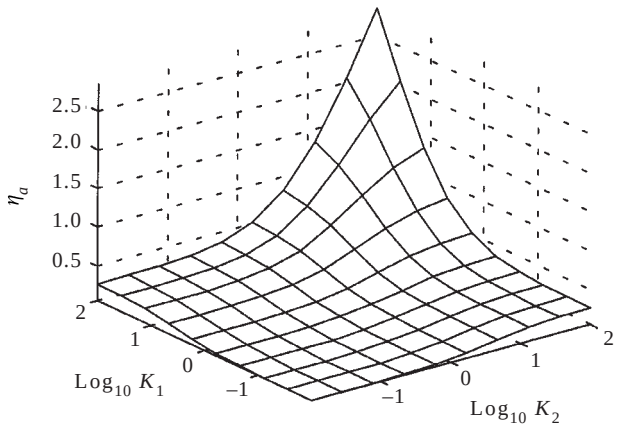

(a)

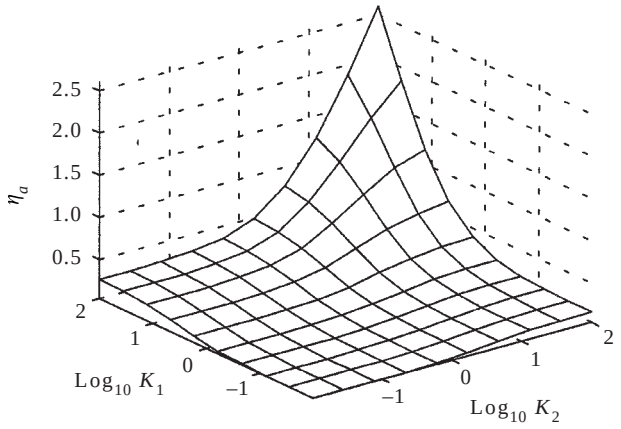

(b)

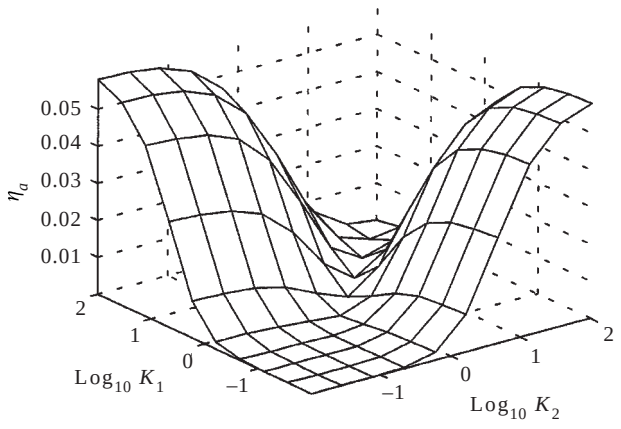

(c)

Figure 11. Active-loss factor versus K_1 and K_2 for $\Gamma = \Gamma_{opt0}$ (optimal control gain for maximizing the system loss factor η_s is used at all points): (a) $A = 0$, (b) $A = 0{\cdot}1$, (c) $A = 0{\cdot}2$.

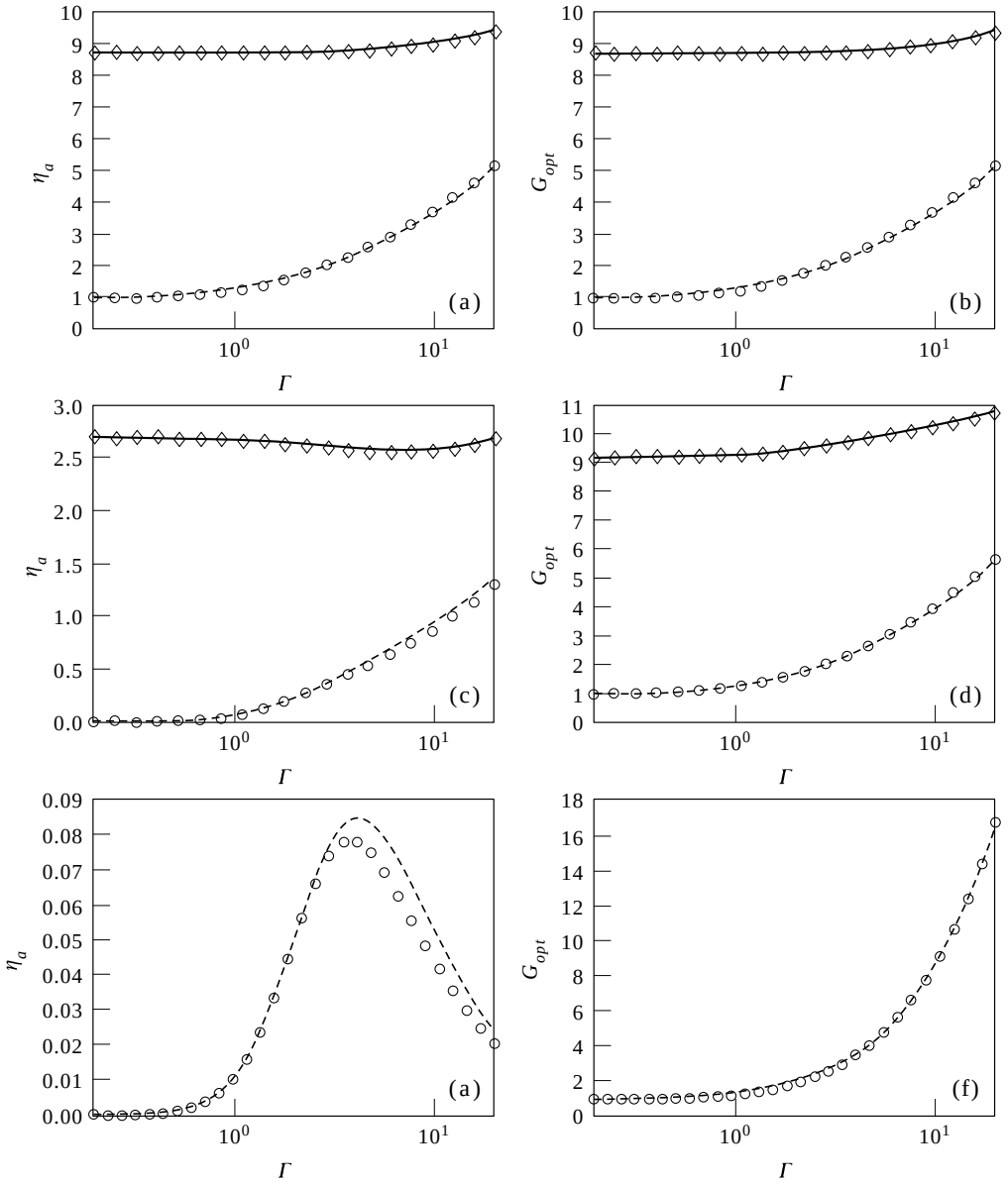

Figure 12. Maximum active-loss factor η_a and its corresponding optimal control gain G_{opt} versus the characteristic length Γ: (a) η_a versus Γ for $A = 0$, (b) G_{opt} versus Γ for $A = 0$, (c) η_a versus Γ for $A = 0{\cdot}1$, (d) G_{opt} versus Γ for $A = 0{\cdot}1$, (e) η_a versus Γ for $A = 0{\cdot}2$, (f) G_{opt} versus Γ for $A = 0{\cdot}2$; ——, $K_1 = K_2 = 100$, $\eta = 1{\cdot}0$; ◇◇◇, $K_1 = K_2 = 100$, $\eta = 0{\cdot}2$; - - -, $K_1 = 100$, $K_2 = 0{\cdot}01$, $\eta = 1{\cdot}0$; ooo, $K_1 = 100$, $K_2 = 0{\cdot}01$, $\eta = 0{\cdot}2$.

(η_p) are different for the different strain fields in the host structure (A) and the different characteristic length Γ of the treatment.

When the strain in the host structure is constant along the length direction ($A = 0$), active control can enhance the passive damping of the EACL treatment. Figure 13 plots the passive loss factor η_p as a function of the control gain G and the strain distribution parameter A for $K_1 = K_2 = 0{\cdot}01$; $K_1 = K_2 = 100$; and

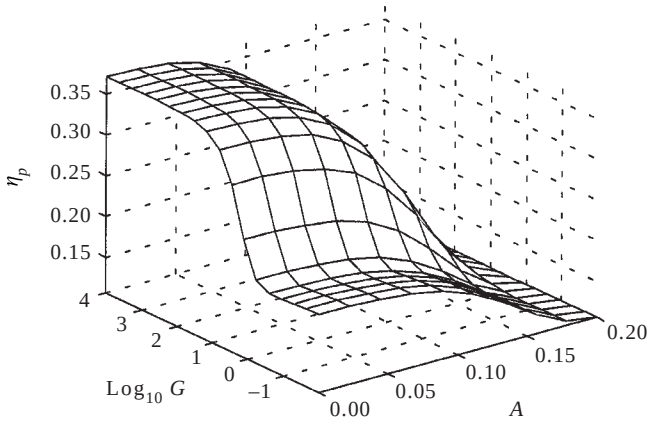

(a)

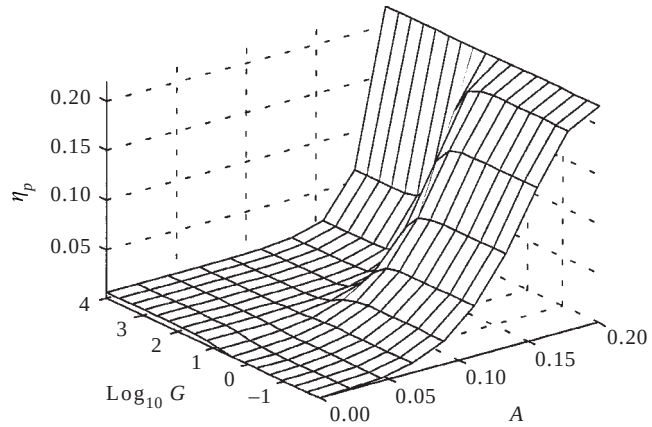

(b)

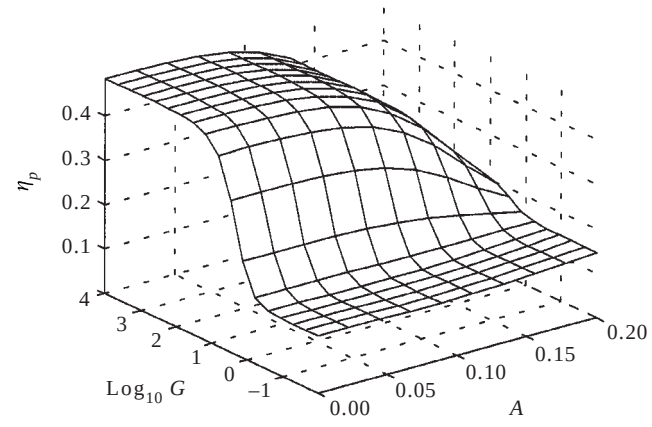

(c)

Figure 13. Passive loss-factor η_p versus gain G and strain distribution parameter A for $\Gamma = \Gamma_{opt0}$: (a) $K_1 = K_2 = 0{\cdot}01$, (b) $K_1 = K_2 = 100$, (c) $K_1 = 100$, $K_2 = 0{\cdot}01$.

$K_1 = 100$, $K_2 = 0{\cdot}01$. It can be seen from the figure that, for a constant strain field in this host structure, η_p increases with the growth of the control gain G, but it saturates when G is sufficiently large. This is again related to the control algorithm used. According to equation (48), when the control gain is so large that the constants C_1 and C_2 approach their limit values, the control will not further change the distribution of u_c and γ, and η_p will thus become insensitive to the increase of the control gain.

It is obvious from Figure 13 that the stiffness distribution of the edge elements will strongly affect the passive damping properties of the EACL treatment. For a constant strain field, to achieve the largest passive damping, the EACL with at least one soft edge element should be used. In Figure 14(a), the passive loss factor η_p is shown versus K_1 and K_2 for $A = 0$. η_p achieves the maximum values when $K_1 = K_2 = 0{\cdot}01$; $K_1 = 100$, $K_2 = 0{\cdot}01$; and $K_1 = 0{\cdot}01$, $K_2 = 100$. This is easy to understand since the active control can increase the shear strain in the VEM layer in these cases. If both ends of the PZT are constrained by the edge elements with high stiffness, the passive loss factor is small, as shown in Figure 14(a).

The EACL with at least one soft edge element not only can provide high passive damping for the constant strain field in the host structure, but also can achieve high passive damping when the strain in the host structure has the same phase ($0 \leqslant A \leqslant 0{\cdot}1$). This is shown clearly in Figures 13(a) and (c). Actually, for each given strain field and characteristic length Γ, an optimal stiffness distribution of the edge elements can be found. Take $A = 0{\cdot}1$ as an example, as shown in Figure 14(b); the EACL with $K_1 = 100$, $K_2 = 0{\cdot}01$ obtains the highest passive loss factor when $\Gamma = \Gamma_{opt0}$. When the strain field in the host structure is anti-symmetrical ($A = 0{\cdot}2$), active control from symmetrical EACL ($K_1 = K_2$) cannot enhance the passive damping, but increasing the active gain in unsymmetrical EACL ($K_1 \neq K_2$) can increase the passive loss factor of the treatment. Since the symmetrical EACL cannot actively control the anti-symmetrical strain field, the shear strain in the VEM layer is also independent of the control gain. Therefore, the control gain G cannot change the passive loss factor of the treatment when K_1 equals K_2, as shown in Figures 13(a) and (b). The passive loss factor is the same as the open-loop loss factor in this case. By changing the stiffness distribution of the edge elements, the anti-symmetrical strain field can be actively controlled by the unsymmetrical EACL, and the passive damping can also be enhanced by the active control, as illustrated in Figure 13(c). Figure 14(c) shows the passive loss factor versus K_1 and K_2. It can be seen that increasing stiffness of any (or both) of the edge elements can improve the overall passive damping of the treatment when the strain field being treated is anti-symmetric. This is because the shear strain in the VEM layer is increased in such scenarios [11]. It is also interesting to note that the enhanced passive damping in the unsymmetrical EACL cases (e.g., $K_1 = 100$, $K_2 = 0{\cdot}01$ or $K_1 = 0{\cdot}01$, $K_2 = 100$) is still lower than the open-loop damping under $K_1 = K_2 = 100$ (Figures 14(c) and 15(c)).

In the above discussion of the effects of the control gain and the stiffness distribution of the edge elements on the passive loss factor of the EACL

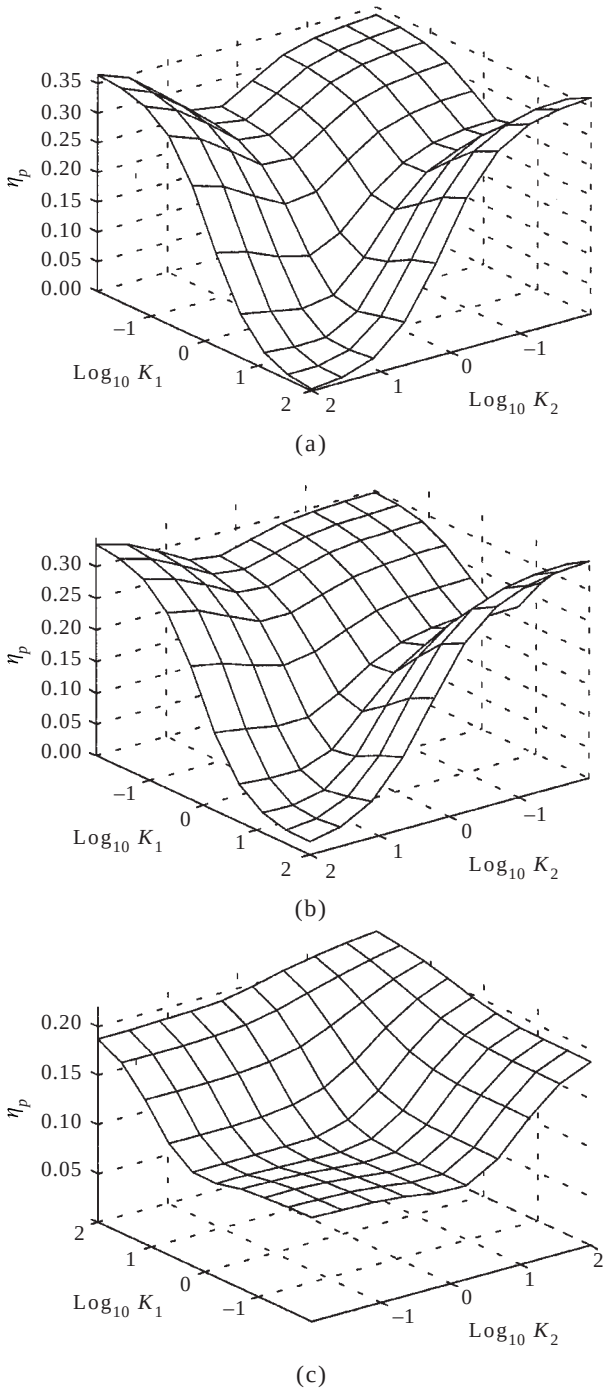

Figure 14. Passive-loss factor η_p versus K_1 and K_2 for $\Gamma = \Gamma_{opt0}$ (optimal control gain for maximizing the system loss factor η_s is used at all points): (a) $A = 0$, (b) $A = 0{\cdot}1$, (c) $A = 0{\cdot}2$.

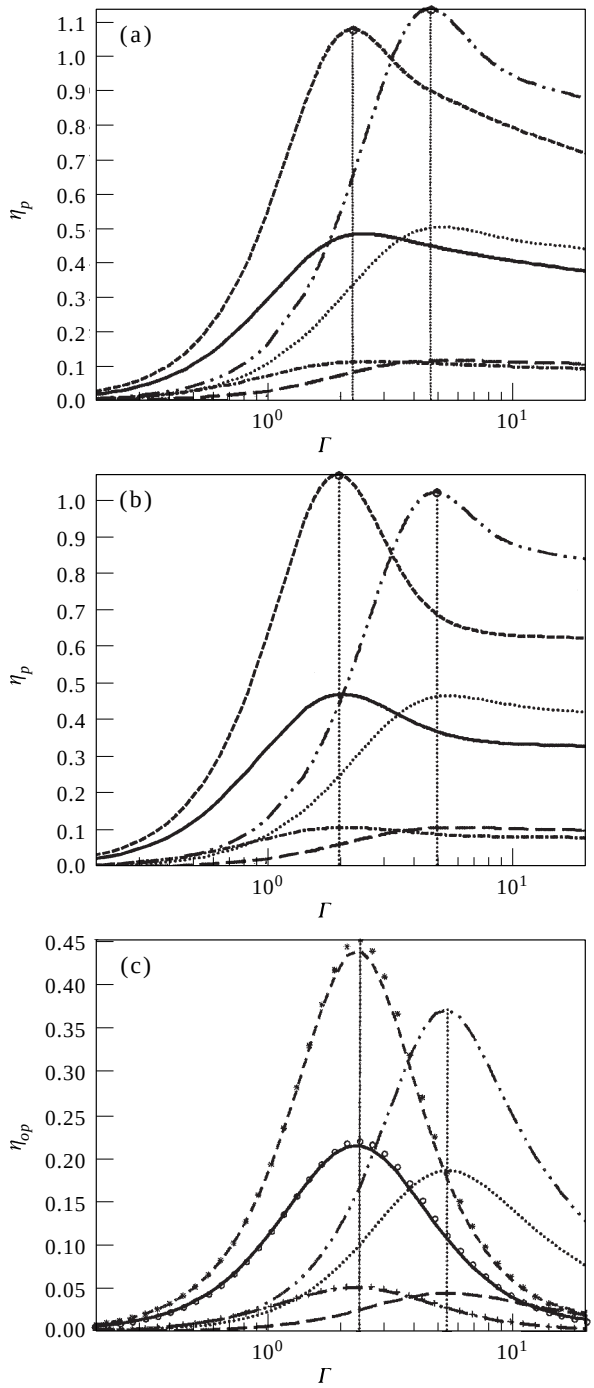

Figure 15. Passive-loss factor η_p versus characteristic length Γ for high control gain; (a) $A = 0$, (b) $A = 0{\cdot}1$, (c) $A = 0{\cdot}2$; ----, $K_1 = 100$, $K_2 = 0{\cdot}01$, $\eta = 5$; ——, $K_1 = 100$, $K_2 = 0{\cdot}01$, $\eta = 1$; -·-·-, $K_1 = 100$, $K_2 = 0{\cdot}01$, $\eta = 0{\cdot}2$; -··-··-, $K_1 = K_2 = 0{\cdot}01$, $\eta = 5$; ·····, $K_1 = K_2 = 0{\cdot}01$, $\eta = 1$; – –, $K_1 = K_2 = 0{\cdot}01$, $\eta = 0{\cdot}2$; ***, $K_1 = K_2 = 100$, $\eta = 5$; ooo, $K_1 = K_2 = 100$, $\eta = 1$; + + +, $K_1 = K_2 = 100$, $\eta = 0{\cdot}2$.

treatment, the characteristic length Γ and the VEM loss factor η are fixed. Figure 15 shows how the passive loss factor changes with the variation of the characteristic length Γ and the VEM loss factor η for high control gain (so that the passive loss factor reaches saturation). Similar to the open-loop system, there is also an optimal characteristic length in the closed-loop system with high control gain to maximize the passive loss factor. When the strain in the host structure has the same sign ($0 \leqslant A \leqslant 0{\cdot}1$), compared to the open-loop system, the optimal characteristic length in the closed-loop system is increased because of the control action. This indicates the characteristic length of the treatment should be designed separately for the open-loop and closed-loop systems. When the strain distribution in the host structure is anti-symmetric ($A = 0{\cdot}2$), the optimal characteristic length for the symmetrical EACL will not change because of the control.

In contrast to the active damping of the treatment, on which the VEM loss factor has almost no effect, the passive damping of the closed-loop system can be improved by using the VEM with a higher loss factor. It can also be observed from the figure that the optimal characteristic length Γ_{opt} remains about the same for the different VEM loss factors.

6.3. HYBRID DAMPING ABILITY OF THE EACL TREATMENT

As defined in equation (44), the system hybrid damping can be derived by summing up the passive and active loss factors. Again, the effects of the control gain G and the stiffness distribution of the edge elements are first discussed for the different strain fields in the host structure. The effects of the characteristic length and the VEM loss factor are then considered.

When the strain along the length of the host structure has the same sign ($0 \leqslant A \leqslant 0{\cdot}1$), active damping dominates in the symmetrical EACL treatment with high-stiffness edge elements, and passive damping dominates when there is at least one very soft edge element in the treatment. As shown in Figure 16, the system loss factor for the symmetrical EACL with the high-stiffness edge elements ($K_1 = K_2 = 100$) is very similar to the active loss factor in Figure 10. The system loss factor of the EACL with at least one soft edge element is very similar to the passive loss factor in Figure 13.

To obtain the maximum system loss factor when the strain has the same sign in the domain of the treatment ($0 \leqslant A \leqslant 0{\cdot}1$), symmetrical EACL with the most rigid edge elements should be used. Figure 17(a) and (b) show the system loss factor versus the stiffness distribution of the edge elements for $A = 0$ and $A = 0{\cdot}1$. Obviously, the higher the stiffness of the edge elements, the greater the system loss factor, since the increase of the active loss factor outweighs the decrease of the passive loss factor (if there is any decrease). In these cases, the selection of the complex characteristic length Γ^* has little effect on the maximum systems loss factor and its corresponding optimal control gain, as shown in Figure 18(a)–(d), since the active loss factor dominates in these situations, and the active loss factor, as shown in Figure 12, is nearly independent of Γ^*.

As A increases (especially from 0·1 to 0·2), using stiff and equal (symmetrical) edge elements to enhance the active damping and system damping of the

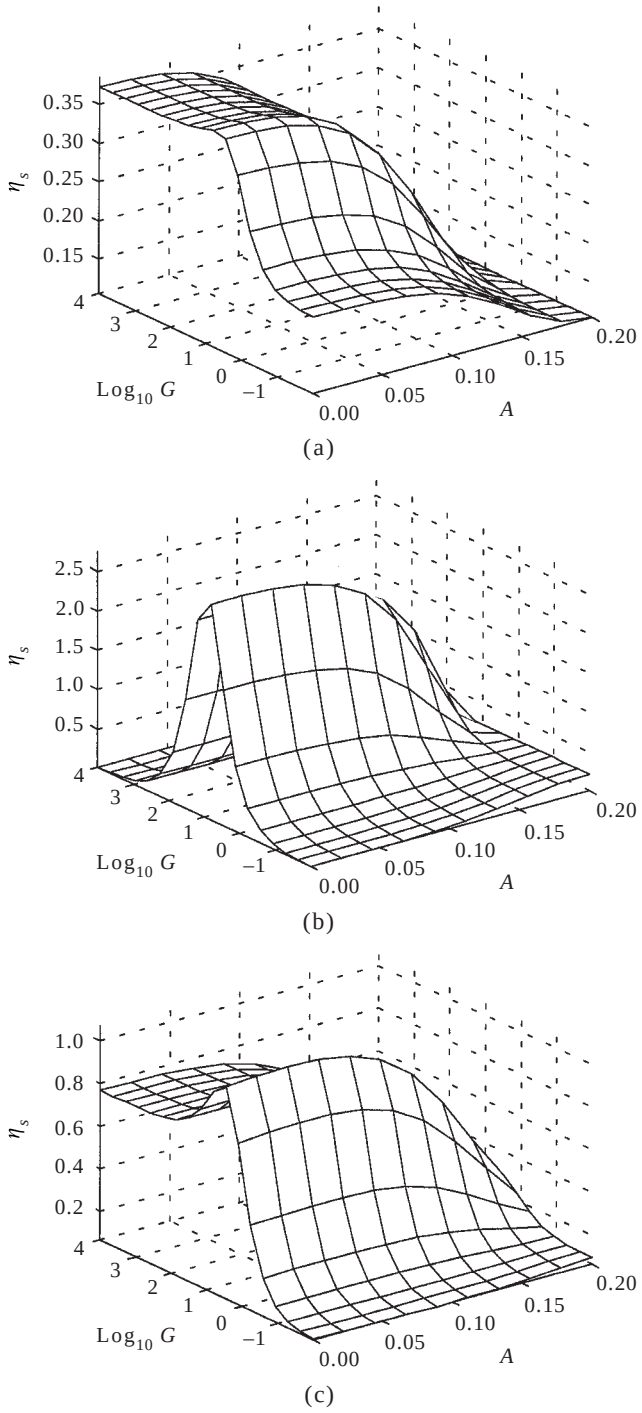

Figure 16. System loss factor η_s versus control gain G and strain distribution parameter A for $\Gamma = \Gamma_{opt0}$: (a) $K_1 = K_2 = 0{\cdot}01$, (b) $K_1 = K_2 = 100$, (c) $K_1 = 100$, $K_2 = 0{\cdot}01$.

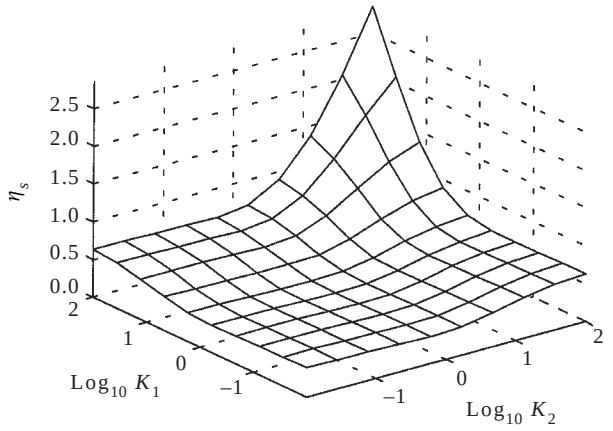

(a)

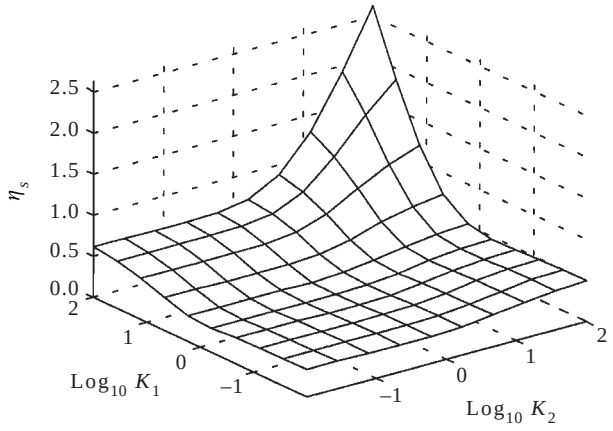

(b)

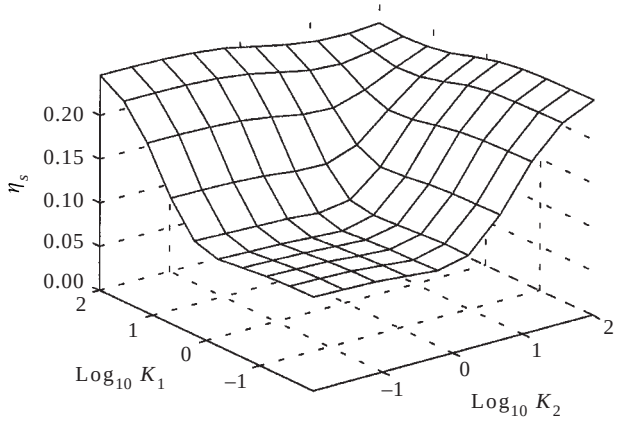

(c)

Figure 17. System loss factor η_s versus K_1 and K_2 for $\Gamma = \Gamma_{opt0}$ (optimal control gain for maximizing the system loss factor η_s is used at all points): (a) $A = 0$, (b) $A = 0{\cdot}1$, (c) $A = 0{\cdot}2$.

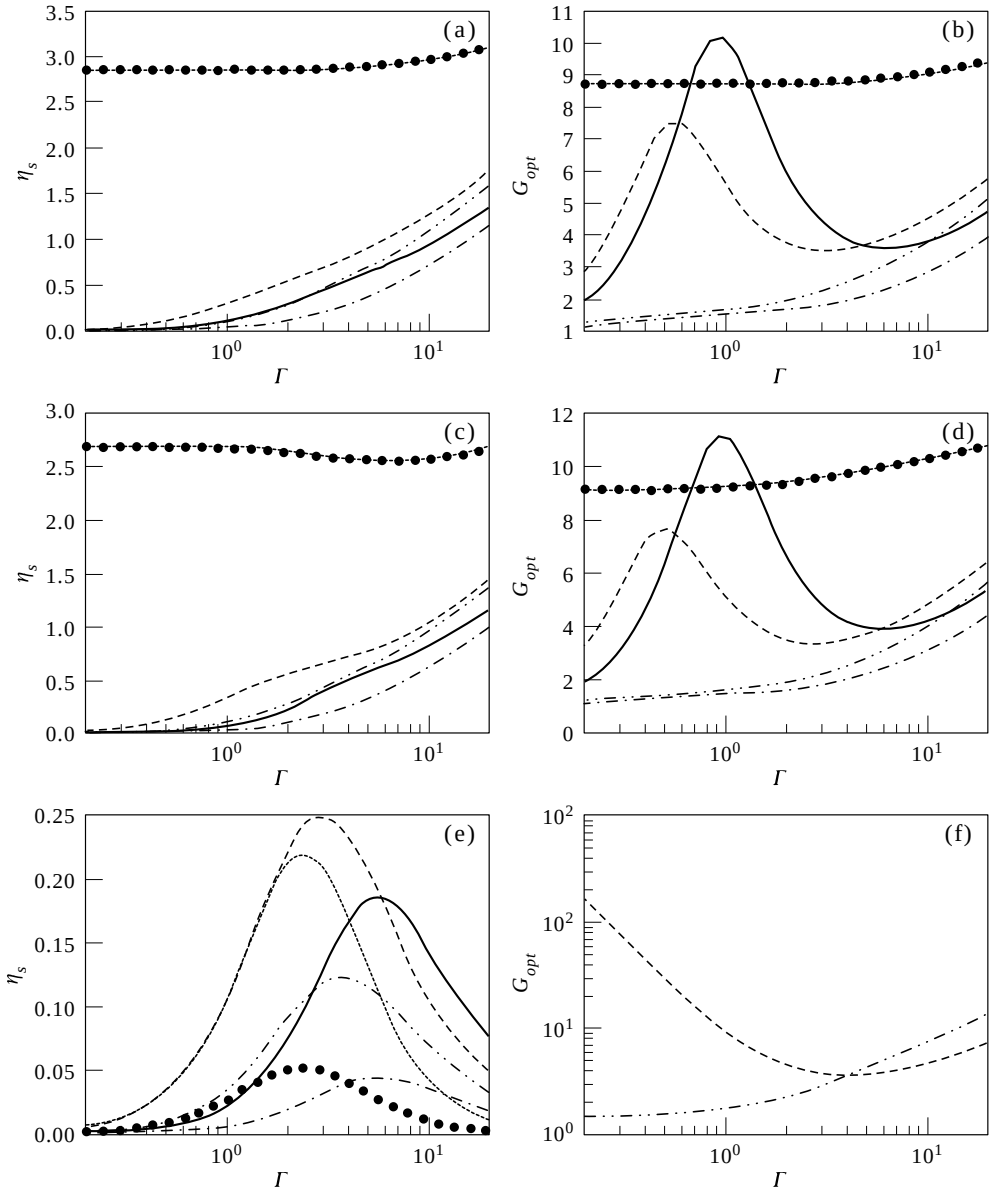

Figure 18. System loss factor η_s and its corresponding optimal control gain G_{opt} versus the characteristic length Γ: (a) η_s versus Γ for $A = 0$, (b) G_{opt} versus Γ for $A = 0$, (c) η_s versus Γ for $A = 0{\cdot}1$, (d) G_{opt} versus Γ for $A = 0{\cdot}1$, (e) η_s versus Γ for $A = 0{\cdot}2$, (f) G_{opt} versus Γ for $A = 0{\cdot}2$; - - - -, $K_1 = 100$, $K_2 = 0{\cdot}01$, $\eta = 1$; ——, $K_1 = K_2 = 0{\cdot}01$, $\eta = 1$; · · · · · · , $K_1 = K_2 = 100$, $\eta = 1$; -·-·-·, $K_1 = 100$, $K_2 = 0{\cdot}01$, $\eta = 0{\cdot}2$; -----, $K_1 = K_2 = 0{\cdot}01$, $\eta = 0{\cdot}2$; ●●●, $K_1 = K_2 = 100$, $\eta = 0{\cdot}2$.

treatment becomes less effective. When the strain field of the host structure is anti-symmetric ($A = -2B$), there is only passive damping in the symmetrical EACL treatment. But in unsymmetrical EACL, there are both passive and active damping. Figure 17(c) shows the system loss factor as a function of the edge element stiffness. Compared with Figure 8(a), it can be seen that the highest point moves from $K_1 = K_2 = 100$ to $K_1 = 100$, $K_2 = 0{\cdot}1$ and $K_1 = 0{\cdot}1$, $K_2 = 100$.

Recall these two points also achieve the highest active loss factor. Therefore, the system damping ability of the EACL treatment on the anti-symmetrical strain field can be improved by selecting unsymmetrical stiffness distribution of the edge elements.

The effectiveness of using the unsymmetrical EACL to enhance the system damping when the strain distribution is anti-symmetric is related to the VEM loss factor and the characteristic length Γ of the treatment. As shown in Figure 18(e), for small VEM loss factor, the system damping ability can be improved significantly by using the unsymmetrical EACL with one stiff edge element. For a high VEM loss factor, however, the improvement is not so prominent when compared with the open-loop system with $K_1 = K_2 = 100$. From the above discussion, it is found that the VEM loss factor has very little effect on the active loss factor, but has significant effects on the passive loss factor. Therefore, for low VEM loss factor, the active damping from the unsymmetrical EACL is far greater than the passive damping. The system loss factor of the closed-loop system can be increased significantly by choosing the unsymmetrical EACL. For high VEM loss factor, the passive damping in the closed-loop system will dominate. The system loss factor of the closed-loop system can only be slightly increased by using unsymmetrical EACL.

7. CONCLUSIONS

This investigation extends the initial work of Liao and Wang [1, 2] on EACL and provides more quantitative and comprehensive results that can be better generalized to design EACL for one-dimensional structures. Closed form solutions to the active, passive and system loss factors are developed. The non-dimensional parameters that affect the damping properties of the treatment are identified and the influences of these parameters on the loss factors are discussed for the open-loop and closed-loop systems.

In the open-loop system, the maximum loss factor and its corresponding optimal characteristic length change with the variation of strain distribution in the host structure. If the strain has the same sign in the domain of the treatment ($0 \leqslant A \leqslant 0{\cdot}1$), the optimal characteristic length for the constant strain distribution can be used and the constraining layer at the high strain end should be constrained by a stiff edge element, while the other edge element should be soft. If the strain distribution is anti-symmetric ($A = 0{\cdot}2$), both ends of the constraining layer should be constrained by stiff edge elements and the corresponding optimal characteristic length should be used. If the strain distribution is such that $0{\cdot}1 < A < 0{\cdot}2$, an optimal stiffness distribution of the edge elements and the corresponding optimal characteristic length can be found for each A.

In the closed-loop system, to obtain the highest system (hybrid) damping ability, the requirements on the stiffness distribution of the edge elements, the optimal control gain, and the treatment characteristic length will be different for different strain distribution in the host structure. If the strain along the host structure is of the same sign ($0 \leqslant A \leqslant 0{\cdot}1$), symmetrical EACL with very stiff

edge elements can significantly improve the system damping ability by mainly improving the active control authority of the treatment. In this case, the optimal control gain has to be used but the complex characteristic length is not important. Unsymmetrical EACL with one stiff edge element and one soft edge element can be used to enhance the passive damping of the treatment. In this case, the complex characteristic length will play an important role. When $0{\cdot}1 < A < 0{\cdot}2$, the optimal stiffness distribution of the edge elements, the optimal control gain and the optimal characteristic length should be found for each given A. When the strain field becomes anti-symmetric ($A = 0{\cdot}2$), symmetrical EACL cannot actively control the structure. The system damping can be improved by using unsymmetrical EACL. The improvement will be related to the VEM loss factor. For a small VEM loss factor, this improvement will be significant. However, the improvement will be very limited for high VEM loss factors.

In practical damping treatment design, open-loop damping guarantees the fail-safe ability of the system, while closed-loop damping quantifies the overall system performance. Based on this study, the following guidelines are developed for the design of the EACL treatment.

The treatment should be on the high strain area since more energy of the treated structure can be dissipated with such arrangement, which is consistent with previous studies about surface damping treatments.

The location and length of the treatment should be such that the strain in the host structure is in phase (has the same sign), which means the treatment does not cover a nodal point of the mode that needs to be controlled. In such a strain field, the closed-loop system damping of the treatment can be significantly higher than the open-loop damping. Depending on the stiffness distribution of the edge elements, the system damping can be mainly from the active part (e.g., $K_1 = K_2 = 100$), passive part (e.g., $K_1 = K_2 = 0{\cdot}01$), or both (e.g., $K_1 = 100$, $K_2 = 0{\cdot}01$; $K_1 = 0{\cdot}01$, $K_2 = 100$).

To fully utilize the EACL's active–passive hybrid characteristics, one design philosophy is to obtain the highest system hybrid damping while maintaining some amount of the open-loop damping for fail-safe purpose. For such a scenario, the key design parameters will be the stiffness distribution of the edge elements, the control gain, and the characteristic length of the treatment. The VEM with the largest loss factor should be used.

From equations (39)–(43), smaller EI and larger Δ should be designed to achieve better damping effect, since EI and Δ only appear in equation (39) which happens to be the denominators of the loss factors. Smaller EI means stiffer constraining layer compared to the host structure. When all the other parameters can be suitably selected, stiffer constraining layer should be used. Larger Δ corresponds to larger offset of the constraining layer from the base structure.

ACKNOWLEDGMENTS

This research is supported by the US Army Research Office, with Dr Gary Anderson as the technical monitor.

REFERENCES

1. W. H. Liao and K. W. Wang 1996 *Journal of Smart Materials and Structures* **5**, 638–648. A new active constrained layer configuration with enhanced boundary actions.
2. W. H. Liao and K. W. Wang 1998 *Journal of Vibration and Acoustics* **120**, 894–900. Characteristics of enhanced active constrained layer damping treatments with edge elements, part 2: system analysis.
3. G. Agnes and K. Napolitano 1993 *Proceedings* 34*th SDM Conference*, 3499–3506. Active constrained layer viscoelastic damping.
4. A. Baz 1993 *Damping* '93 *Conference IBB*, 1–23. Active constrained layer damping.
5. A. Baz 1997 *Journal of Smart Materials and Structures* **6**, 360–368. Optimization of energy dissipation characteristics of active constrained layer damping.
6. S. C. Huang, D. J. Inman and E. M. Austin 1996 *Journal of Smart Materials and Structures* **5**, 301–313. Some design considerations for active and passive constrained layer damping treatments.
7. W. H. Liao and K. W. Wang 1997 *ASME Journal of Vibration and Acoustics* **119**, 563–572. On the active–passive hybrid control actions of active constrained layers.
8. W. H. Liao and K. W. Wang 1997 *Journal of Sound and Vibration* **207**, 319–334. On the analysis of viscoelastic materials for active constrained layer damping treatments.
9. I. Y. Shen 1997 *ASME Journal of Vibration and Acoustics* **119**, 192–199. A variational formulation, a work-energy relation and damping mechanisms of active constrained layer treatments.
10. R. Plunkett and C. T. Lee 1970 *Journal of the Acoustical Society of America* **48**, part 2, 150–161. Length optimization for constrained viscoelastic layer damping.
11. Y. Liu and K. W. Wang 1998 *Proceedings of SPIE on Smart Structures and Materials* **3327**, 61–72. Enhanced active constrained layer damping treatment with symmetrically and non-symmetrically distributed edge elements.
12. K. B. Demoret and P. J. Torvik 1995 *ASME Design Engineering Technical Conference* **84**, 719–726. Optimal length of constrained layers on a substrate with linearly varying strain.

APPENDIX: NOMENCLATURE

b	width of the Beam, VEM, or PZT
d_{31}	piezoelectric constant
h_c, h_s, h_b	thickness of PZT, VEM and base beam, respectively
h	distance from the mid-plane of the base beam to the mid-plane of the PZT
i	$\sqrt{-1}$
u_c, u_b	average longitudinal displacements of PZT and base beam, respectively
w	transverse displacement
x	position co-ordinate along the base beam length
z	position co-ordinate along the base beam thickness
γ	shear strain in VEM
σ_c	axial stress of PZT
δ	displacement between the edge element and the corresponding bound of PZT

τ	shear stress of VEM
η	loss factor of VEM
η_{op}	open-loop loss factor
η_a, η_p, η_s	active, passive and hybrid loss factor of EACL treatment, respectively
Λ	free strain of PZT
ε	axial strain of the beam
ω	vibration frequency in radians
A, B, C	constants used in the assumption of beam strain or displacement field
C_1, C_2	constants determined by the boundary conditions of the PZT
A_c, A_s, A_b	cross section area of PZT, VEM and base beam, respectively
E_c, E_b	Young's Modulus of PZT and base beam, respectively
EI	ratio of the bending stiffness of the host structure and the PZT
G_s	complex shear modulus of VEM
G	non-dimensional control gain
G_1	storage modulus of the VEM
I_c, I_b	moment of inertia of PZT and base beam, respectively
K_{eq1}, K_{eq2}	stiffness of the edge elements at $x = 0$ and $x = L$, respectively
K_g	control gain
L	length of the PZT
V	control voltage
W_a, W_p	energy dissipated per cycle by active control and passive damping, respectively
W_s	maximum strain energy stored in the PZT, VEM, edge elements and beam section beneath VEM.
K_1, K_2	non-dimensional stiffness of the edge elements at $x = 0$ and $x = L$, respectively
$\bar{x}$	non-dimensional position co-ordinate along base beam length defined as x/L
$\bar{z}_c$	non-dimensional position co-ordinate along the PZT thickness defined as $(z-h)/L$
$\bar{z}$	non-dimensional position co-ordinate along base beam thickness defined as z/L
θ_c	non-dimensional thickness of PZT defined as h_c/L
θ_b	non-dimensional thickness of the host beam defined as h_b/L
θ_s	non-dimensional thickness of VEM defined as h_s/L
θ_h	non-dimensional length between the mid-planes of the base beam and the PZT defined as h/L
$\bar{u}_c$	non-dimensional longitudinal displacement of PZT defined as u_c/L
$\bar{u}_b$	non-dimensional longitudinal displacement of base beam defined as u_b/L
$\bar{w}$	non-dimensional transverse displacement defined as w/L
Γ^*	complex characteristic length of EACL treatment defined as $\Gamma^* = \sqrt{G_s^* L^2/E_c h_c h_s}$

Γ characteristic length or the magnitude of the complex characteristic length Γ^*

Γ_{opt0} optimal characteristic length of PCL without edge elements for constant strain field

Γ_{opt1} optimal characteristic length of PCL with $K_1 = 100(\infty)$ and $K_2 = 0$ for constant strain field

Γ_{opt2} optimal characteristic length of PCL with $K_1 = K_2 = 100(\infty)$ for anti-symmetric strain field

Δ non-dimensional offset distance of the PZT from the neutral axis of the beam defined as h/h_c